Communication of Stabilizing Energy between Substructures of a Protein†

Richard Kristinsson and Bruce E. Bowler*

Department of Chemistry and Biochemistry, 2190 E. Iliff Avenue, University of Denver, Denver, Colorado 80208-2436

Received August 27, 2004; Revised Manuscript Received December 1, 2004

ABSTRACT: Thermodynamic communication between protein substructures has been investigated by determining the stabilizing effect of mutations at position 52 in the least stable, N-yellow, substructure of cytochrome *c* on the second least stable, Red, and most stable, Blue, substructures of the protein. A Lys 73 → His (H73) variant of iso-1-cytochrome *c*, containing these mutations was used to measure the stability of the Red substructure of cytochrome *c* through the pH and guanidine hydrochloride (gdnHCl) dependence of the His 73-mediated alkaline conformational transition. The stability of the Blue substructure was measured by global unfolding with gdnHCl and increased by 1 to 3.5 kcal/mol versus the H73 variant. The data demonstrate that the increase in stability of the Red substructure is similar to the increase in global stability, consistent with upward propagation of stabilizing energy from less (N-yellow) to more stable (Red and Blue) protein substructures. The result also supports sequential rather than independent unfolding of the N-yellow and Red substructures of cytochrome *c*. The data indicate that a leucine at position 52 alters the nature of partial unfolding of the Red substructure, a surprising effect for a single-site mutation. For all variants, the thermodynamics of formation of the Lys 79 alkaline state, which does not unfold the entire Red substructure, shows less stabilization of the portion of the protein unfolded relative to the stabilization of the Blue substructure, indicating that propagation of energy between substructures is somewhat disrupted when unfolding does not correspond to a natural substructure.

Understanding the forces that stabilize proteins has been an important focus of studies on protein folding (*1*, *2*). Recent work indicates that proteins may use specific pathways to communicate conformational energy (*3*). Given this observation and the fact that a number of single domain proteins have several cooperative units or substructures (*4*, *5*), it is of interest to determine how energy is communicated between protein substructures.

The cooperative substructures of cytochrome *c* from horse heart have been extensively studied by hydrogen deuterium exchange (HX)[1] methods (*6*−*11*). These studies have revealed five cooperative folding units of different stabilities, as shown in Figure 1. Although detailed studies have not been carried out on cytochrome *c* from other species, HX and ^{15}N relaxation data on the yeast iso-1-cytochrome *c* (*12*−*14*) are qualitatively consistent with the substructures defined for horse heart cytochrome *c* (*10*). Thus, cytochrome *c* is well-suited for studies on intersubstructure interactions.

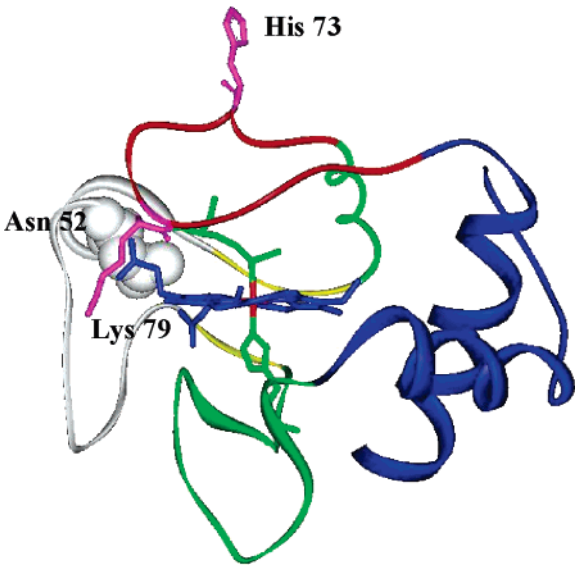

FIGURE 1: Structure of yeast iso-1-cytochrome *c* showing the substructures determined for the horse protein using the color scheme of Englander and co-workers (*10*). From least to most stable, the substructures are N-yellow (shown in white, residues 40−57), Red (residues 71−85), Yellow (residues 37−39 and 58−61), Green (60's helix and 20's−30's loop), and Blue (N- and C-terminal helices). The heme is shown as a blue stick model. His 73 and Lys 79 are shown as magenta stick models. The heme ligands, His 18 and Met 80, are shown as green stick models. Asn 52 is show in white as a space-filling model. The structure of oxidized iso-1-cytochrome *c* (2ycc) was used. The figure was created with WebLab ViewerLite (v. 4.0) software.

† Acknowledgment is made to the donors of the Petroleum Research Fund (38865-AC4, B.E.B.), administered by the American Chemical Society, for partial support of this work. Partial support was also provided by NIH Grant GM57635-02 (B.E.B.). The Applied Photophysics π*-180 Spectrometer was purchased with NIH Grant 1 S10 RR16632-01. R.K. acknowledges support from the Partners in Scholarship Program at the University of Denver.

* To whom correspondence should be addressed. Phone: (303) 871-2985. Fax: (303) 871-2254. E-mail: bbowler@du.edu.

[1] Abbreviations: H73, variant of iso-1-cytochrome *c* carrying a Lys 73 to His mutation; X52 H73, iso-1-cytochrome *c* variant carrying a mutation of Asn 52 to amino acid X, where X is a one letter amino acid abbreviation, as well as the Lys 73 to His mutation; mutations are denoted by abbreviations of the form N52A, which for example indicates that Asn 52 in the wild-type protein has been converted to alanine; WT, wild type; CD, circular dichroism; gdnHCl, guanidine hydrochloride; HX, hydrogen−deuterium exchange; PUF, partially unfolded form.

10.1021/bi048141r CCC: $30.25
Published on Web 01/28/2005

On the basis of equilibrium thermodynamics, protein molecules must unfold and refold under native conditions as defined by the Boltzmann distribution. During unfolding and refolding of proteins, the individual folding units of the protein might be expected to follow a stability-dependent pathway, where the lowest energy substructure must unfold before the substructure of second lowest conformational energy, and so forth. For cytochrome *c*, the native state HX data are consistent with this mechanism (*6*, *7*). This result leads to the conclusion that substructures of higher stability are dependent on the unfolding of lower stability substructures, if they are to unfold. For cytochrome *c*, using the substructure designations of Englander and co-workers, the following set of equilibria would be expected for unfolding of cytochrome *c* under native conditions, where from least to most stable, the substructures of cytochrome *c* are N-yellow (N), Red, (R), Yellow, (Y), Green (G), and Blue (B) (see Figure 1).

$$\mathrm{NRYGB} \overset{K_N}{\rightleftharpoons} \mathrm{nRYGB} \overset{K_R}{\rightleftharpoons} \mathrm{nrYGB} \overset{K_Y}{\rightleftharpoons} \mathrm{nryGB} \overset{K_G}{\rightleftharpoons} \mathrm{nrygB} \overset{K_N}{\rightleftharpoons} \mathrm{nrygb}$$

Due to the sequential nature of the unfolding equilibria, stabilization of any substructure must be communicated into the surrounding substructures of higher conformational energy. Thus, a stabilizing mutation in the N-yellow substructure of cytochrome *c* would be expected to stabilize all higher energy substructures. Upward propagation of stabilization energy has been observed for the stabilizing mutation D10A in RNase HI (*15*) and by strengthening the heme iron to Met 80 bond (by reduction of Fe^{3+} to Fe^{2+}) in the Red substructure of cytochrome *c* (*7*). On the other hand, the available data indicate that a decrease in the stability of a higher energy substructure is not communicated to lower energy substructures (*16*). These experimental results are consistent with thermodynamic models for propagation of binding interactions in proteins (*17*). These models predict that propagation of stabilization energy from a low-stability substructure or domain to a higher energy substructure or domain is very efficient when a ligand binds to the low-stability substructure or domain. The opposite, downward propagation of stabilization energy when a ligand binds to the more stable part of a protein, is inefficient.

In this laboratory, we have developed a Lys 73 → His (H73) variant of iso-1-cytochrome *c* that uses a heme ligand exchange reaction (His 73 replacing Met 80 in the sixth coordination site of the heme) to stabilize a partially unfolded form (PUF) of iso-1-cytochrome *c* (*18*, *19*). Analysis of the free energy of partial unfolding as a function of guanidine hydrochloride (gdnHCl) concentration and temperature yields an *m*-value (*20*) and ΔC_p (*21*), respectively, which are consistent with the properties observed for unfolding of the Red substructure of cytochrome *c* (*6*). The K73H mutation replaces one of the lysines involved in the alkaline conformational transition of iso-1-cytochrome *c* (*22*). The pH dependence of the thermodynamics (*20*) and kinetics (*23*) of formation of the PUF of the H73 variant is consistent with it being related to the alkaline conformational transition of cytochrome *c* (*22*, *24*). Recent HX experiments have established a relationship between unfolding the Red substructure and the formation of the alkaline state of cytochrome *c* (*25*). Thus, the PUF stabilized by replacement of Met 80 with His 73 in the sixth coordination site of the heme of the H73 variant of iso-1-cytochrome *c* provides a good model, both structurally and thermodynamically, for unfolding of the Red substructure of cytochrome *c*. Since the partial unfolding of the H73 variant can be monitored by a straightforward absorbance-detected pH titration, this variant provides a facile means to monitor the effects of mutations in adjacent substructures on the stability of the Red substructure of cytochrome *c*.

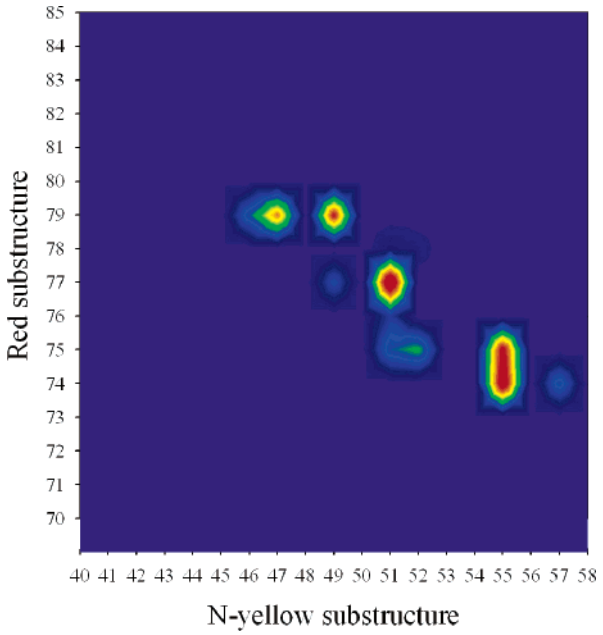

FIGURE 2: Second least stable (Red) substructure versus least stable (N-yellow) substructure contact map for oxidized iso-1-cytochrome *c*. The numbers on the axes correspond to sequence position. The contour levels are from 0 (blue) to 35 Å^2 (red) in 5 Å^2 increments. The contact surface areas were generated with CSU (Contacts of Structural Units) software (*30*) (http://bip.weizmann.ac.il/oca-bin/lpccsu) using the Protein Databank file 2ycc as input. Crystallographically defined water molecules, such as water 166, which is near Asn 52, are not currently included in the calculations carried out by CSU. So, surface area calculations reflect only contacts between side chains, backbone atoms, and the heme prosthetic group.

Mutations at Asn 52 (N52) of iso-1-cytochrome *c*, located in the least stable N-yellow substructure of cytochrome *c*, have large effects on the global stability of iso-1-cytochrome *c* (*26*−*28*). The global stability can be decreased by up to 1.0 kcal/mol and increased by up to 5.0 kcal/mol relative to the wild-type (WT) protein depending on the amino acid substitution at position 52. Thus, effects on stability can be monitored over a wide range. The surface area contact of N52 with the Red substructure is 20.2 ± 0.6 Å^2, as determined from X-ray structure data for oxidized iso-1-cytochrome *c* (*29*) using CSU software (*30*). The total contact surface area between the least stable substructure and the second least stable substructure is 274 ± 3 Å^2 (Figure 2). Thus, there is a small amount of direct contact between N52 and the Red substructure and a reasonable amount of surface area contact between the two substructures providing for direct physical communication of stability from the N-yellow to the Red substructure.

Here we report the effects of mutations of Asn 52 to Ala, Val, Thr, Leu, and Ile in the N-yellow substructure on the

global stability (unfolding of the Blue substructure) versus the stability of the Red substructure (as monitored by partial unfolding of the H73 variant driven by His 73 ligation to the heme), allowing analysis of the effects of a broad range of stabilization energies on two different substructures. We find that stability is distributed equally to the Red and Blue substructures, consistent with upward propagation of stability by sequential unfolding of the protein. This result also demonstrates that the N-yellow substructure unfolds prior to and not independently of the Red substructure. Previous results could not directly distinguish whether these two substructures unfolded independently or sequentially (*10*). Finally, data for the Leu 52 variant indicate that single-site mutations can alter the nature of protein substructures.

MATERIALS AND METHODS

Preparation of Iso-1-cytochrome c Variants. Site-directed mutagenesis on the iso-1-cytochrome *c* gene (*CYC1*) carrying the K73H and C102S mutations (*18*) was carried out using single-stranded template DNA derived from either the pRS425/CYC1 phagemid (*18*) (N52A mutation) or the pRS/C7.8 phagemid (*31*) (all other mutations). The C102S mutation puts a serine at position 102 to prevent dimerization of the protein during physical studies. Mutations of Asn 52 to Ala, Thr, Val, Leu, or Ile were made using the method of unique restriction site elimination (*31*, *32*), using the *Sac*I+II− (N52A mutation) or *Sac*I−II+ (all other mutations) selection primers (*31*) to eliminate, respectively, the unique *Sac*II or the unique *Sac*I restriction enzyme sites upstream from the *CYC1* gene in these phagemids. Mutagenesis reactions were transformed into *Mut*S (BMH 71−18) *Escherichia coli* cells, the isolated DNA cut with either the *Sac*I (*Sac*I−II+ primer) or *Sac*II (*Sac*I+II− primer) restriction enzyme, to linearize nonmutant DNA, and the resulting DNA transformed into TG-1 *E. coli* cells. DNA isolated from single TG-1 colonies (Wizard SV+ DNA miniprep kit from Promega Corp., Madison, WI) was sequenced using a Beckman CEQ8000 automated DNA sequencer to screen for the desired mutations.

Mutated pRS425/CYC1 and pRS/C7.8 phagemid DNAs were transformed into *Saccharomyces cerevisiae* GM-3C-2 cells by the LiCl method (*33*). Transformed yeast were characterized by phenotypic screening (tests for functional cytochrome *c*), a curing procedure (*34*) (demonstrates phagemid-based expression), and rescue of the phagemid (*35*) followed by resequencing (ensures that selective conditions used to express iso-1-cytochrome *c* in yeast have not caused additional mutations).

Isolation and purification of iso-1-cytochrome *c* variants from transformed GM-3C-2 cells were carried out as previously described (*34*, *36*).

Oxidation of Iso-1-cytochrome c Variants. Prior to all experiments, iso-1-cytochrome *c* variants were oxidized for 1 h at 4 °C using an excess of $K_3Fe(CN)_6$. The oxidized protein was run through a G-25 size exclusion column to separate the oxidizing agent from the protein. The column was equilibrated to and run with a buffer appropriate to the experiment to be performed on the oxidized protein. The protein concentration and degree of oxidation were then determined spectrophotometrically, as previously described (*36*).

GdnHCl Denaturation Monitored by CD Spectroscopy. Global protein stability was determined by gdnHCl denaturation monitored by CD spectroscopy. The experiments were done in 20 mM Tris, 40 mM NaCl at pH 7.5. A 7.0 M gdnHCl stock solution was made containing this buffer. The concentration of the gdnHCl stock solution was determined using refractive index measurements (*37*). Denaturations were done at 25 ± 0.1 °C using Jasco J500C or Applied Photophysics π*-180 spectropolarimeters at a protein concentration of 2 and 4 μM, respectively.

When using the Jasco J500C, we performed all titrations manually, as previously described (*38*). Unfolding titrations on the π*-180 spectrometer were performed using a two-syringe Hamilton MICROLAB 500 titration unit. An 850 μL volume of 4 μM native protein in 20 mM Tris, 40 mM NaCl, pH 7.5, was denatured by titrating in fully denatured protein (4 μM concentration) in 7 M gdnHCl, 20 mM Tris, 40 mM NaCl, pH 7.5, using the Hamilton titration unit equipped with two 250 μL syringes. Since the concentration of the protein in both syringes is identical, the concentration of the protein remains 4 μM throughout the gdnHCl unfolding titration. One syringe pulled out the desired amount of protein solution from the sample cuvette, while the other injected the same amount of denatured protein stock into the sample cuvette. The software on the π*-180 spectrometer was used to calculate the volume removed from and replaced into the sample cuvette to achieve the next desired [gdnHCl] given the starting gdnHCl concentration (0 M), the initial sample volume (850 μL), and the gdnHCl concentration in the fully denatured protein solution (usually near 7 M) as input data. In general, the denaturant concentration steps were 0.1 M in the native and denatured baseline regions and 0.05 M in the unfolding transition region of the gdnHCl denaturation titration. A stirring speed of 180 rpm and a stirring time of 100 s were used after each addition of the concentrated gdnHCl solution to ensure complete mixing and equilibration of the sample. The ellipticity was then monitored at 222 and 250 nm (subtracted from the 222 nm signal as a baseline).

The ellipticity data as a function of gdnHCl concentration were fit to eq 1 (*39*), using nonlinear least-squares methods (SigmaPlot, version 7.1, SSPS, Inc.). In eq 1, θ_N° is the ellipticity of native protein at 0 M gdnHCl, θ_D° is the ellipticity of denatured protein at 0 M gdnHCl, m_D is the [gdnHCl] dependence of the denatured-state ellipticity, m is the gdnHCl concentration dependence of the free energy of unfolding, and $\Delta G_u(H_2O)$ is the free energy of unfolding extrapolated to 0 M gdnHCl.

$$\theta = \frac{\theta_N^\circ + \{(\theta_D^\circ + m_D[\text{gdnHCl}])e^{(m[\text{gdnHCl}]-\Delta G_u(H_2O))/RT}\}}{1 + e^{(m[\text{gdnHCl}]-\Delta G_u(H_2O))/RT}} \quad (1)$$

A linear free energy relationship is assumed in eq 1, as given by eq 2 (*37*). Use of nonlinear least-squares methods to simultaneously fit the pre- (θ_N°) and posttransition (θ_D°,m_D) baselines and the transition region ($\Delta G_u(H_2O)$, m) fits the raw data directly and thus provides a better evaluation of the parameters than when baseline regions are chosen manually and fit separately from the transition region (*40*).

$$\Delta G_u = \Delta G_u(H_2O) - m[\text{gdnHCl}] \quad (2)$$

Partial Unfolding by GdnHCl Monitored at 695 nm. The loss of native Met 80−iron ligation at pH 7.5 was monitored at 695 nm (*41*) using a Beckman DU640 spectrophotometer while increasing the gdnHCl concentration in order to partially unfold the protein. From these data, an assessment of the stability of the least stable substructure was obtained. Absorbance at 750 nm was used as the background wavelength for the experiments, which were done in 20 mM Tris, 40 mM NaCl at pH 7.5 with 180−190 μM protein concentration at 25 ± 0.1 °C and a sample volume of 500 μL. At each concentration of gdnHCl, 70 μL was transferred to a microcuvette and the absorbance was measured. To raise the [gdnHCl] for the next data point in the titration, a calculated amount of the 70 μL sample in the microcuvette was returned to the titration solution and then equal volumes of 7 M gdnHCl and a 2× protein stock (360−380 μM protein concentration, both the gdnHCl and protein stocks contain 20 mM Tris, 40 mM NaCl, pH 7.5 buffer) were added to the titration solution to return its volume to 500 μL. The procedure maintains constant protein concentration throughout the gdnHCl titration. The 695 nm data were fit to eq 3 using nonlinear least-squares methods (SigmaPlot, version 7.1, SSPS, Inc.), where A_{695} is the absorbance at 695 nm at a given concentration of gdnHCl, $A^{\circ}_{695,N}$ is the absorbance at 695 nm of the native protein at 0 M gdnHCl due to Met 80−iron ligation, $A^{\circ}_{695,D}$ is the absorbance at 695 nm of the partially unfolded/denatured protein with the Met 80−iron ligation disrupted extrapolated to 0 M gdnHCl, m_D is the [gdnHCl] dependence of the partially unfolded/denatured-state absorbance at 695 nm, and the other parameters are as defined in eq 1.

$$A_{695} = \frac{A^{\circ}_{695,N} + \{(A^{\circ}_{695,D} + m_D[\mathrm{GdnHCl}])e^{\{(m[\mathrm{GdnHCl}]-\Delta G_u(H_2O))/RT\}}\}}{1 + e^{\{(m[\mathrm{GdnHCl}]-\Delta G_u(H_2O))/RT\}}} \quad (3)$$

Alkaline Conformational Transition Monitored by Absorbance Spectroscopy. Studies were carried out at protein concentrations of 190−200 μM in 100 mM NaCl at 25 ± 0.1 °C. The sample was prepared by diluting 1 mL of 2× protein stock (380−400 μM protein in 200 mM NaCl) with 1 mL of sterile ddH_2O. The pH was measured with a Corning pH meter 220 with a Corning Semimicro Ag/AgCl Combination Probe (part no. 476156). The initial spectrum was taken when the pH of the protein sample was approximately 4.5. The pH was adjusted by adding equal volumes of the 2× protein stock and of a NaOH solution of appropriate concentration to the titration solution. By carrying out the pH titration in this manner, the protein concentration remains constant (190−200 μM) throughout the titration. The titration solution was mixed with a 1000 μL pipet, and then the pH and the absorption spectrum (600−750 nm) were recorded. When pH 11 was reached, the protein solution was adjusted back to pH 4.5 with 3 M HCl and an equal volume of 2× protein stock. The sample volume was then adjusted to 2 mL, and 2*x* μL of the sample was removed and replaced with 1*x* μL of concentrated gdnHCl stock and 1*x* μL of 2× protein stock, where the value of *x* in the volumes is calculated so as to bring the gdnHCl concentration to the desired level for the next alkaline transition measurement. The pH titration was then repeated as described above, except 1 μL of 3×-concentrated gdnHCl stock (for example, if the gdnHCl concentration for the pH titration is 1.0 M, the concentration of the 3×-concentrated gdnHCl stock would be 3.0 M) was added in addition to 0.5 μL of NaOH and 1.5 μL of the 2× protein stock for each pH increment. This method of titration keeps both the protein and gdnHCl concentration constant throughout the titration. pH titrations at additional concentrations of gdnHCl were carried out with the same sample, as described above, to obtain the pH and gdnHCl dependence of partial unfolding for each variant.

The A_{695} versus pH data were fit to eq 4 or 5 (*20*), which are consistent with the equilibrium model described in Results, where A_{695} is the absorbance at 695 nm as a function of pH, A_N is the absorbance at 695 nm of the native state of the protein, A_{alk} is the absorbance at 695 nm of the alkaline conformer of the protein, pK_C(H73) is the conformational p*K* ($-\log(K_C)$, where K_C is the equilibrium constant for the conformational change) for the alkaline transition involving His 73−heme ligation, pK_C(K79) is the conformational p*K* for the alkaline transition involving Lys 79−heme ligation, and p$K_H(T_1H^+)$ and p$K_H(T_2H^+)$ are, respectively, the pK_as for the ionizable groups mediating these transitions. Data were fit to these equations using nonlinear least-squares methods (SigmaPlot, version 7.1, SSPS, Inc.). Equation 4 was used when both the His 73- and Lys 79-mediated alkaline conformational transitions were evident from the data. Equation 5 was used when only the Lys 79-mediated alkaline conformational transition was observed.

$$A_{695} = \frac{A_N + \left(A_{alk}\left(\frac{10^{-pK_C(H73)}}{1 + 10^{pK_H(T_1H^+)-pH}} + \frac{10^{-pK_C(K79)}}{1 + 10^{pK_H(T_2H^+)-pH}}\right)\right)}{1 + \left(\frac{10^{-pK_C(H73)}}{1 + 10^{pK_H(T_1H^+)-pH}} + \frac{10^{-pK_C(K79)}}{1 + 10^{pK_H(T_2H^+)-pH}}\right)} \quad (4)$$

$$A_{695} = \frac{A_N + \left(A_{alk}\left(\frac{10^{-pK_C(K79)}}{1 + 10^{pK_H(T_2H^+)-pH}}\right)\right)}{1 + \left(\frac{10^{-pK_C(K79)}}{1 + 10^{pK_H(T_2H^+)-pH}}\right)} \quad (5)$$

RESULTS

Global Unfolding of Position 52 Variants. GdnHCl denaturation of the X52 H73 variants (in the nomenclature X52 H73, X52 indicates mutation of Asn 52 to an amino acid X, where X is the one letter abbreviation for the amino acid and H73 indicates a Lys 73 to His mutation) monitored by CD spectroscopy was used to determine global stability. Data for two variants, H73 A52 and H73 I52, are illustrated in Figure 3. The mutations at position 52 have significant effects on the global stability of H73 iso-1-cytochrome *c*. Relative to the H73 variant, all X52 H73 variants show increases in the free energy of unfolding in aqueous solution, $\Delta G_u(H_2O)$, and the gdnHCl concentration at the midpoint of the titration, C_m (see Table 1).

Results from gdnHCl denaturation monitored at 695 nm are also shown in Figure 3. The data show that as the global stability of the X52 H73 variant increases, the gdnHCl unfolding monitored at 695 nm progressively moves toward coincidence with the CD-monitored unfolding. The absor-

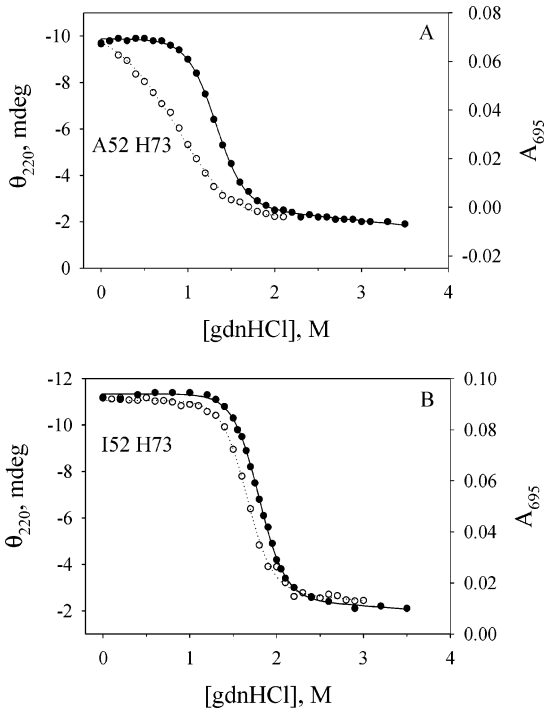

FIGURE 3: Plots of absorbance at 695 nm (○) versus gdnHCl concentration and of ellipticity at 220 nm versus gdnHCl concentration (●) for (A) A52 H73 and (B) I52 H73 iso-1-cytochromes *c*. Data were collected in 20 mM Tris, 40 mM NaCl at pH 7.5, 25 ± 0.1 °C, and protein concentrations of 180−190 μM at 695 nm and of 2 μM for ellipticity at 220 nm. Titrations were carried out as described in Materials and Methods. The solid (θ_{220}) and dotted (A_{695}) curves are nonlinear least-squares fits of the data to eqs 1 and 3, respectively, in Materials and Methods.

bance at 695 nm monitors the presence of the Met 80−heme iron bond (*41*). The degree to which the loss of 695 nm absorbance precedes loss of ellipticity at 220 nm provides an indication of the degree to which partial unfolding occurs prior to global unfolding of cytochrome *c* variants (*18*, *19*, *42*). GdnHCl denaturation was carried out at pH 7.5 so the His 73 residue of each variant would be predominantly deprotonated, maximizing the population of the partially unfolded intermediate stabilized by His 73−heme ligation (*18*, *19*). For the A52 H73 variant (Figure 3A), a fit of the A_{695} versus [gdnHCl] data to eq 3 (Materials and Methods) gives $\Delta G_u(H_2O) = 1.6 \pm 0.1$ kcal/mol and $m = 1.6 \pm 0.1$ kcal mol^{-1} M^{-1}). The *m*-value is similar to that observed for the gdnHCl unfolding of the H73 variant monitored at 695 nm (refs *18*, *20*, ~1.7 kcal mol^{-1} M^{-1}) and that for the Red substructure of horse cytochrome *c* (ref *6*, 1.6 kcal mol^{-1} M^{-1}). The almost complete separation of the A_{695} and CD-monitored gdnHCl unfolding titrations allows reasonable parameters for partial unfolding to be extracted for the A52 H73 variant from the A_{695} versus [gdnHCl] data. For the I52 H73 variant (Figure 3B), the A_{695} and CD-monitored gdnHCl unfolding titrations are nearly coincident. The fit of the A_{695} versus [gdnHCl] data to eq 3 (Materials and Methods) yields $\Delta G_u(H_2O) = 6.4 \pm 0.3$ kcal/mol and $m = 3.8 \pm 0.2$ kcal mol^{-1} M^{-1}. These values are very similar to the ones obtained from the CD versus [gdnHCl] data (Table 1), indicating that the A_{695} versus [gdnHCl] data is monitoring global unfolding in this case and thus partial unfolding does not occur in advance of global unfolding. For the T52 H73 variant (Figure S1, Supporting Information), the deviation between the A_{695} and CD unfolding data is intermediate between what is observed for the A52 H73 and I52 H73 variants (Figure 3), and the A_{695} versus [gdnHCl] data yield thermodynamic parameters that primarily reflect partial unfolding ($\Delta G_u(H_2O) = 2.5 \pm 0.1$ kcal/mol and $m = 2.3 \pm 0.2$ kcal mol^{-1} M^{-1}). The *m*-value obtained from the A_{695} versus [gdnHCl] data is increased relative to the A52 H73 variant due to increased overlap of the partial (A_{695}) and global (CD) unfolding transitions (Figure S1). For the V52 H73 variant (Figure S1), the deviation between the A_{695} and CD unfolding data is similar to what is observed for the I52 H73 variant (Figure 3B), and the thermodynamic parameters obtained from the A_{695} versus [gdnHCl] data ($\Delta G_u(H_2O) = 5.4 \pm 0.3$ kcal/mol and $m = 4.2 \pm 0.4$ kcal mol^{-1} M^{-1}) also reflect global unfolding (see Table 1). Although the global stabilities of the I52 H73 and L52 H73 variants are similar (Table 1), the deviation between the A_{695} and CD unfolding data for the L52 H73 variant (Figure S1) is more than what is observed for the I52 H73 variant (Figure 3B), and there is a slow decrease in A_{695} prior to the main unfolding transition. The thermodynamic parameters obtained from the A_{695} versus [gdnHCl] data for the L52 H73 variant indicate that partial (A_{695}) and global (CD) unfolding are overlapping transitions ($\Delta G_u(H_2O) = 4.6 \pm 0.2$ kcal/mol and $m = 2.8 \pm 0.3$ kcal mol^{-1} M^{-1}), not unlike the behavior of the T52 H73 variant.

In comparing the thermodynamic parameters in Table 1 for the X52 H73 variants relative to the H73 variant (*18*), an increase in the *m*-value is also generally observed (Table 1), and it tracks well with the relative behavior of the A_{695} versus the CD-monitored gdnHCl unfolding transitions. The trend in *m*-values for the CD-monitored data is consistent with less population of intermediates during global unfolding for more stable variants (*18*, *19*, *43*). The behavior of the L52 H73 variant is somewhat at odds with this trend, indicating that the N52L mutation may have altered the nature of the partial unfolding mediated by His 73.

When the changes in stability, $\Delta\Delta G$, due to mutations at position 52 in the presence of the His 73 mutation are compared to previously reported $\Delta\Delta G$ values for the same variants in the WT background (*28*), in general, the trends in stability are similar (Table 1). The one clear exception is the Ala 52 mutation. This difference could result from the use of Ala at position 102 in the studies in the WT background (*28*) (position 102 is Cys in the naturally occurring iso-1-cytochrome *c*) instead of the Ser used at position 102 in this work. We find that $\Delta\Delta G$ in our WT-(C102S) background for the Ala 52 mutation is similar to that reported between the A52 H73 and H73 variants (Redzic, Grover, and Bowler, unpublished results), supporting this interpretation.

pH and GdnHCl Dependence of the Alkaline Conformational Transition. In previous work, we have shown that monitoring the alkaline transition of the H73 variant of iso-1-cytochrome *c* as a function of [gdnHCl] provides an accurate means of accessing the thermodynamics of partial unfolding (*20*) and thus of the stability of the Red substructure. The 695 nm charge-transfer band, due to heme−Met 80 ligation, was monitored as a function of pH for each of the variants at a series of gdnHCl concentrations. In each case, the highest [gdnHCl] used was chosen to be ~0.2 M less than that required for the onset of global unfolding to

Table 1: Thermodynamic Parameters for GdnHCl Unfolding of Iso-1-cytochrome *c* Variants Monitored by Ellipticity at 220 nm, pH 7.5, and 25 ± 0.1 °C[a]

variant	$\Delta G_u(H_2O)$ (kcal/mol)	*m* (kcal mol^{-1} M^{-1})	C_m (M)	$\Delta\Delta G$ (kcal/mol) versus H73 (C102S)	$\Delta\Delta G$[b] (kcal/mol) X52 (C102A) versus WT (C102A)
WT[c]	5.77 ± 0.40	5.11 ± 0.36	1.13		
H73[d]	3.68 ± 0.19	3.20 ± 0.18	1.15		
A52 H73	4.51 ± 0.17	3.49 ± 0.09	1.29	0.83 ± 0.36	2.97
T52 H73	5.02 ± 0.09	3.83 ± 0.06	1.31	1.34 ± 0.28	1.90
V52 H73	6.15 ± 0.15	4.27 ± 0.11	1.44	2.47 ± 0.34	2.02
L52 H73	6.96 ± 0.35	3.83 ± 0.14	1.82	3.28 ± 0.54	4.73
I52 H73	7.15 ± 0.15	3.97 ± 0.09	1.80	3.47 ± 0.34	4.10

[a] Thermodynamic parameters are the average of values from three independent experiments. Error is the standard deviation. [b] Data are from Table 2, ref *28*. [c] Data are from ref *39*. [d] Data are from ref *19*.

ensure that only partial unfolding was measured without interference from global unfolding. All experiments have been carried out in the presence of 100 mM NaCl to allow comparison with previous data (*20*). Although the solution conditions are somewhat different from those used for global unfolding measurements (20 mM Tris, 40 mM NaCl, pH 7.5), previous data indicate that this difference in solution conditions has a negligible effect on the thermodynamics of partial unfolding (cf. references *20* and *21*).

Figure 4 shows the alkaline conformational transition for the A52 H73, I52 H73, and L52 H73 variants of iso-1-cytochrome *c* at different concentrations of gdnHCl. As observed previously for the H73 variant (*20*), the data for the A52 H73 variant are biphasic and can be fit to the partitioned equilibrium shown below (the equilibrium parameters are defined in Materials and Methods).

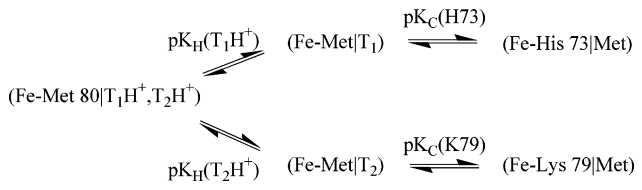

In the data in Figure 4A, the low-pH phase corresponds to formation of the His 73 alkaline conformer and the high-pH phase corresponds to formation of the Lys 79 alkaline conformer. Absorbance at 695 nm monitors the loss of heme−Met 80 ligation as a function of pH irrespective of whether Met 80 ligation is replaced by His 73 or Lys 79 ligation to the heme during the alkaline conformational transition. So, a biphasic transition, as observed for the A79 H73 variant (Figure 4A), indicates that the low-pH alkaline transition driven by His 73−heme ligation does not go to completion. Loss of Met 80−heme ligation is only completed at high pH when Lys 79 binds to the heme. In biphasic alkaline transitions, the equilibrium constant for the low-pH phase, pK_C(H73), can be accurately determine from the leveling out of A_{695} at the end of the low-pH phase. The pK_H(T_1H^+) for the ionizable group triggering the low-pH phase can also be accurately determined when the alkaline transition is biphasic. Recent pH jump kinetic studies confirm that His 73 is the ionizable group (pK_H(T_1H^+)), which controls the position of the equilibrium for the alkaline transition involving His 73−heme ligation for the H73 iso-1-cytochrome *c* variant (*23*). The solid curves in Figure 4A are fits of the A52 H73 data to the above model using eq 4 (Materials and Methods). The low-pH phase of the alkaline transition for the A52 H73 variant (Figure 4) and for the T52 H73 variant (Figure S2, Supporting Information) is sensitive to increases in gdnHCl concentration. The loss of heme−Met 80 ligation, due to formation of the His 73 alkaline conformer (unfolding of the Red substructure), clearly goes further to completion as the denaturant concentration increases. Similar behavior was observed for the H73 variant (*20*).

As the stabilizing effect of the position 52 mutation in the least stable substructure increases, the population of the His 73 alkaline conformer becomes less prominent. In the least stable variants, A52 H73 (Figure 4A) and T52 H73 (Figure S2), biphasic transitions are observed. For the more stable variants, V52 H73 (Figure S2) and I52 H73 (Figure 4B), biphasic alkaline transitions are not seen at any [gdnHCl]. Due to the lack of the low-pH phase, only the lower branch of the partitioned equilibrium is needed to fit the data. The solid curves in Figure 4B are fits of the I52 H73 data to this simpler equilibrium using eq 5 (Materials and Methods). Surprisingly, one of the most stable variants, L52 H73, shows a biphasic alkaline transition above 0.3 M gdnHCl (Figure 4C), consistent with population of the His 73 alkaline conformer in this variant. This observation indicates that the Leu 52 substitution somehow alters the nature of this conformational transition, as suggested by the A_{695} versus [gdnHCl] data described above (Figure S1).

The thermodynamic parameters obtained from fitting the alkaline conformational transition data for all X52 H73 variants are collected in Table 2. As expected, the pK_C(H73) values are more positive (less favorable equilibrium) for the A52 H73, T52 H73, and L52 H73 variants than for the H73 variant, consistent with stabilization of the Red substructure by the position 52 mutations. Similarly, the pK_C(K79) values are less negative than those for the H73 variant, indicating that the portion of the protein unfolded by the Lys 79 alkaline conformer is also stabilized by the position 52 mutations. The magnitude of pK_C(K79) progressively becomes less negative as the global stability of the variant increases (Table 2). All pK_C values become less positive or more negative as the [gdnHCl] is increased, consistent with the expected destabilization by gdnHCl of the Red substructure (pK_C(H73)) or part of the protein (pK_C(K79)) unfolded in the alkaline conformer. For the variants where a low-pH phase is observed, the pK_H(T_1H^+) is reasonably consistent with a histidine as observed for the H73 variant (*20*). The pK_H(T_1H^+) values also vary in no regular way with [gdnHCl], a general observation for histidine (*44*, *45*). As the conforma-

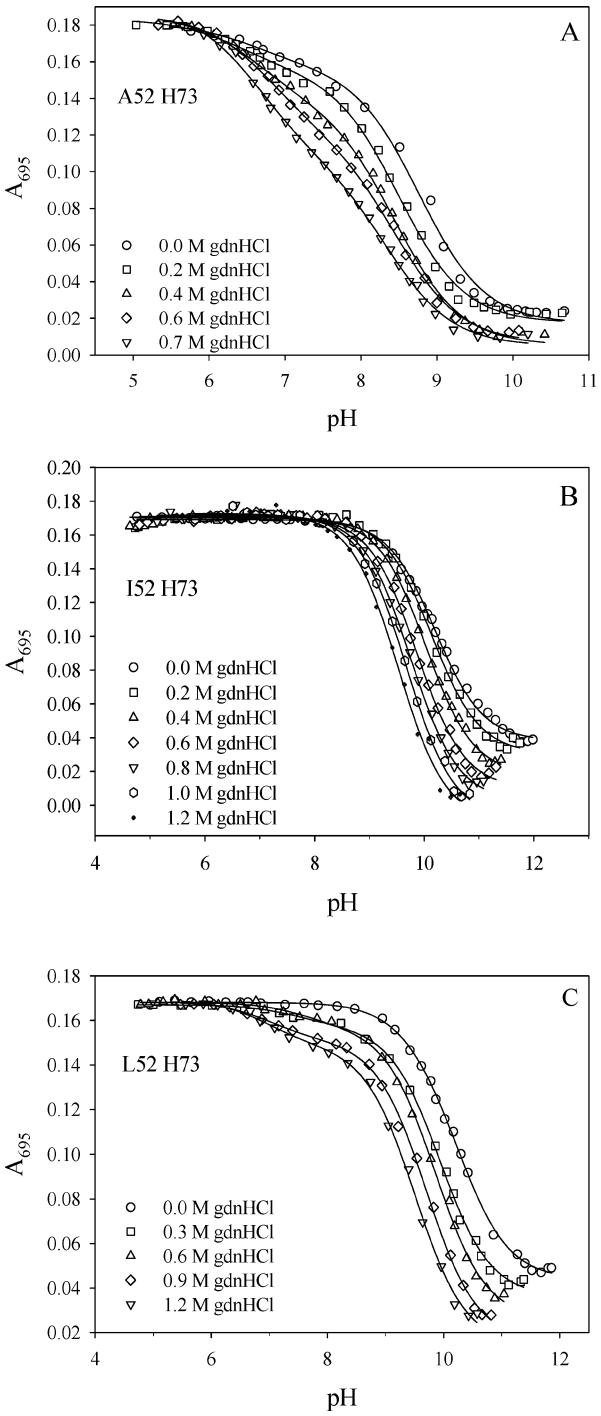

FIGURE 4: Plots of absorbance at 695 nm versus pH for (A) A52 H73, (B) I52 H73, and (C) L52 H73 iso-1-cytochromes *c* at different concentrations of guanidine hydrochloride. Data were collected in 0.1 M NaCl at 25 ± 0.1 °C at protein concentrations of 190−200 μM. Titrations were carried out as described in Materials and Methods. The solid curves for the A52 H73 and L52 H73 (0.3 to 1.2 M gdnHCl) data are fits to eq 4 in Materials and Methods, where $pK_H(T_2H^+) = 10.8$, the value obtained from kinetic experiments for the K79 alkaline state (*22*). The solid curves for the I52 H73 and L52 H73 (0 M gdnHCl) data are fits to eq 5 in Materials and Methods, where $pK_H(T_2H^+) = 10.8$.

tional accessibility of the alkaline transition involving His 73−heme ligation decreases, it is more difficult to fit data to the partitioned equilibrium (eq 4) and $pK_H(T_1H^+)$ becomes more variable and less well defined (see parameters for T52 H73 in Table 2).

Table 2: Thermodynamic Parameters for the Alkaline Conformational Transition of Variant Iso-1-cytochromes *c* as a Function of [GdnHCl] at 25 °C[a]

variant	[gdnHCl] (M)	pK_C(H73)	$pK_{H1}(T_1H^+)$	pK_C(K79)
H73[b]	0	0.28 ± 0.01	6.6 ± 0.1	−2.18 ± 0.11
	0.1	0.14 ± 0.02	6.7 ± 0.2	−2.24 ± 0.04
	0.2	0.02 ± 0.08	6.7 ± 0.2	−2.39 ± 0.14
	0.3	−0.09 ± 0.01	6.7 ± 0.1	−2.39 ± 0.10
A52 H73	0	0.80 ± 0.09	6.6 ± 0.4	−2.09 ± 0.04
	0.2	0.71 ± 0.05	6.4 ± 0.2	−2.38 ± 0.03
	0.4	0.48 ± 0.03	6.7 ± 0.1	−2.47 ± 0.03
	0.6	0.28 ± 0.03	7.0 ± 0.1	−2.52 ± 0.03
	0.7	0.13 ± 0.03	6.9 ± 0.1	−2.69 ± 0.04
T52 H73	0	(1.9 ± 0.5)	(7 ± 2)	−1.74 ± 0.02
	0.3	1.22 ± 0.20	6.7 ± 0.8	−1.89 ± 0.04
	0.6	0.74 ± 0.25	7.5 ± 0.5	−2.10 ± 0.07
	0.8	0.65 ± 0.11	7.2 ± 0.4	−2.17 ± 0.05
V52 H73	0.0			−1.14 ± 0.05
	0.3			−1.31 ± 0.05
	0.5			−1.51 ± 0.04
	0.7			−1.56 ± 0.06
L52 H73	0			−0.50 ± 0.01
	0.3	1.19 ± 0.09	7.5 ± 0.4	−0.82 ± 0.03
	0.6	1.15 ± 0.08	7.6 ± 0.3	−0.92 ± 0.03
	0.9	0.94 ± 0.04	7.0 ± 0.2	−1.11 ± 0.03
	1.2	0.85 ± 0.04	7.0 ± 0.2	−1.32 ± 0.03
I52 H73	0.0			−0.48 ± 0.02
	0.2			−0.56 ± 0.02
	0.4			−0.70 ± 0.01
	0.6			−0.89 ± 0.02
	0.8			−1.00 ± 0.02
	1.0			−1.11 ± 0.03
	1.2			−1.28 ± 0.03

[a] Parameters obtained from fitting A_{695} versus pH data to eqs 4 and 5 in Materials and Methods. [b] Data for the H73 variant are from ref *20*.

DISCUSSION

Structural Properties of Partially Unfolded Forms of X52 H73 Variants. Denaturant *m*-values obtained from the [gdnHCl] dependence of a protein unfolding transition provide important insight into the extent of structural disruption associated with the unfolding transition, since the magnitude of the *m*-value correlates with the extent of exposure of buried hydrophobic surface coincident with the unfolding transition (*46*). The pK_C(H73) and pK_C(K79) values are plotted versus [gdnHCl] for several of the X52 H73 variants in Figure 5. The [gdnHCl] dependence of pK_C shows good linearity for both the His 73 (pK_C(H73))- and Lys 79 (pK_C(K79))-driven conformational transitions. In general, the steepness of the plot is greater for the His 73 alkaline conformational transition than for the Lys 79 alkaline conformational transition, the exception being the L52 H73 variant. The *m*-values and the pK_C in the absence of denaturant, $pK_C(0)$, obtained from fitting the data for all variants to a linear free energy relationship, are tabulated in Table 3. For the A52 H73 and T52 H73 variants, the *m*-value obtained for the His 73 alkaline conformational transition is similar to the value obtained for the parent H73 protein (see Table 3), indicating that the extent of partial unfolding in this conformational transition has not been significantly perturbed by these mutations at position 52. In the case of the A52 H73 variant, where partial (A_{695}) and global (CD) unfolding are reasonably well-separated, the *m*-value of 1.6 ± 0.1 kcal mol^{-1} M^{-1}) obtained from the A_{695} versus [gdnHCl] data (Figure 3A) is identical to the *m*-value

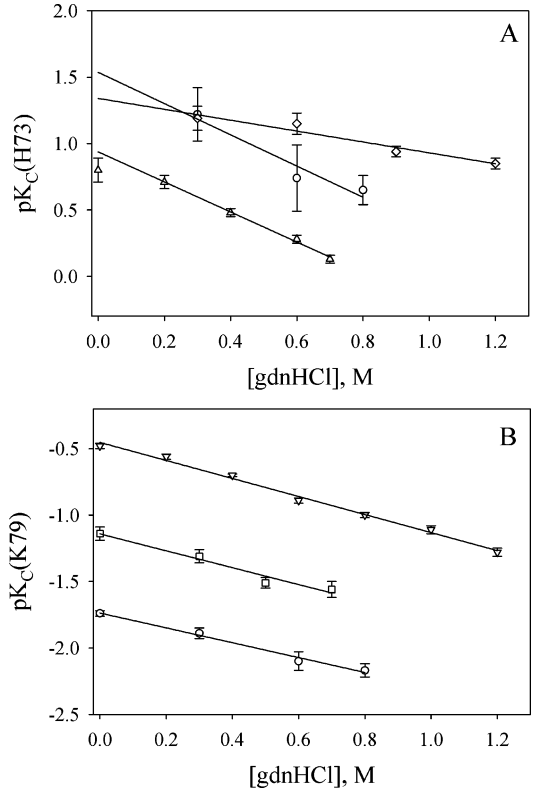

FIGURE 5: Plots of the guanidine hydrochloride concentration dependence of (A) pK_C(H73) for the A52 H73 (△), T52 H73 (○), and L52 H73 (◇) variants and of (B) pK_C(K79) for I52 H73 (▽), V52 H73 (□), and T52 H73 (○) variants. The plots are derived from the data in Table 2. The solid lines are fits to a linear free energy relationship: $pK_C = pK_C(0) - \{m/(\ln(10)RT)\}[\text{gdnHCl}]$, where R is the universal gas constant and T is temperature in degrees Kelvin. The parameters from these fits are collected in Table 3.

obtained from the [gdnHCl] dependence of the His 73-mediated alkaline conformational transition. The *m*-value obtained for formation of the His 73-mediated alkaline conformer is also similar to that reported for unfolding of the Red substructure of cytochrome *c* (ref *6*, 1.6 kcal mol^{-1} M^{-1}).

For the V52 H73 (Figure S2) and I52 H73 (Figure 4B) variants, no low-pH phase due to formation of the His 73 alkaline conformer is observed. In these cases, the large increase in global stability due to the V52 and I52 mutations appears to result in strong stabilization of the Red substructure. Given the small *m*-value (∼1.6 kcal mol^{-1} M^{-1}) for the conformational transition that unfolds the Red substructure, even at the highest [gdnHCl] used in the pH titration experiments, the decrease in the stability of the Red substructure due to gdnHCl is not sufficient to allow the His 73 alkaline conformer to be observed for the V52 H73 and I52 H73 variants. Surprisingly, the L52 H73 variant, despite the large increase in its global stability (Table 1), appears to form a His 73-mediated alkaline conformer (Table 2). Interestingly, the *m*-value observed for the His 73-mediated alkaline conformational transition is much lower than that observed for the H73, A52 H73, and T52 H73 variants (Figure 5A and Table 3), indicating that the L52 mutation has modified the nature of the His 73 alkaline conformation.

For the Lys 79 alkaline conformational transition, the *m*-values observed are generally between 0.8 and 1.0 kcal mol^{-1} M^{-1} (Table 3). These values are similar to those observed for the WT and H73 variants in previous work (*20*) (see Table 3). Given that Met 80 is much closer to Lys 79 than to His 73, much greater structural disruption is expected for a heme ligand at position 73 than for one at position 79 for the alkaline state of cytochrome *c* (*22*). Also, given the smaller *m*-value, the Lys 79 alkaline conformational transition does not appear to correspond to partial unfolding of the Red substructure of cytochrome *c*, although it presumably unfolds a portion of this substructure.

Propagation of Stabilization from the N-Yellow to the Red and Blue Substructures. The pK_C(0) values are readily converted to free energy of partial unfolding in aqueous solution, $\Delta G_u(H_2O)$, and are given in Table 3 for each of the X52 H73 variants. These values can then be used to calculate $\Delta\Delta G$ for partial unfolding for each of the X52 H73 variants relative to the H73 variant (Table 4), allowing comparison with $\Delta\Delta G$ for global unfolding (Blue substructure). In terms of global stability, all variants are stabilized relative to the H73 variant, with stabilization energies, $\Delta\Delta G_{global}$, ranging from 0.8 to 3.5 kcal/mol. For the A52 H73 and T52 H73 variants, the $\Delta\Delta G$ values for formation of the His 73 alkaline conformer, $\Delta\Delta G_{His\ 73}$, are 0.9 and 1.7 kcal/mol, respectively. Since formation of this alkaline conformer corresponds to unfolding of the Red substructure, the data indicate that the Blue and Red substructures of cytochrome *c* are stabilized, within error, by a similar amount by mutations at position 52 in the N-yellow substructure (Table 4). This result is consistent with upward propagation of stabilization energy from the lowest energy, N-yellow, substructure to higher energy substructures of cytochrome *c*, as has been observed for intersubstructure communication of stabilization energy in other cases (*7*, *15*). This type of propagation of stabilization energy is expected for sequential unfolding of cytochrome *c* as outlined in the Introduction.

We note that the $\Delta\Delta G_{global}$ values for the X52 H73 variants relative to the H73 variant may be slightly overestimated since the CD-monitored global unfolding is predominately from the His 73 alkaline conformer for the H73 variant (see Figure 6 in ref *18*). However, the difference in stability between the native and His 73 alkaline conformer of the H73 variant (Table 3) is small and within the error of the $\Delta\Delta G$ values, so we have made no correction for this small deviation.

For the V52 H73 and I52 H73 variants, no His 73 alkaline conformer is observable at the highest [gdnHCl] used (0.7 and 1.2 M, respectively). A quick calculation can be used to determine if this observation is consistent with $\Delta\Delta G_{global}$ also being similar to $\Delta\Delta G_{His73}$ for these two variants. If we use an *m*-value of 1.6 kcal mol^{-1} M^{-1} for formation of the His 73 alkaline conformer and assume that the Red substructure unfolded in this alkaline conformer has been stabilized by $\Delta\Delta G_{global}$ for these variants, then ΔG for the His 73 alkaline conformer relative to the native state at the highest [gdnHCl] used to monitor the alkaline transition for each variant can be calculated as $\Delta G_{His73} = 0.37 + \Delta\Delta G_{global} - 1.6[\text{gdnHCl}]$ (where 0.37 is the stability of the His 73 alkaline conformer relative to the native state in the H73 variant). For the V52 H73 (at 0.7 M gdnHCl) and I52 H73 (at 1.2 M gdnHCl) variants, ΔG_{His73} is ∼1.7 and 1.9 kcal/mol, respectively. So, the maximal population of the His 73 alkaline state for each of these variants would be 3−5% at the highest accessible [gdnHCl], and thus it would not be

Table 3: Thermodynamic Parameters Derived from the GdnHCl Concentration Dependence of the Alkaline Conformational Transition for Variant Iso-1-cytochromes *c* at 25 °C[a]

	His 73 alkaline conformer			Lys 79 alkaline conformer		
variant	pK_C(0)	*m* (kcal mol^{-1} M^{-1})	ΔG_u (H_2O) (kcal/mol)	pK_C(0)	*m* (kcal mol^{-1} M^{-1})	ΔG_u (H_2O) (kcal/mol)
WT[b]				-2.19 ± 0.02	1.09 ± 0.09	-2.98 ± 0.03
H73[b]	0.27 ± 0.01	1.68 ± 0.07	0.37 ± 0.01	-2.18 ± 0.03	1.1 ± 0.3	-2.97 ± 0.05
A73 H73[c]	0.94 ± 0.03	1.54 ± 0.07	1.28 ± 0.04	-2.15 ± 0.06	1.01 ± 0.18	-2.93 ± 0.08
T52 H73[c]	1.5 ± 0.2	1.6 ± 0.4	2.1 ± 0.3	-1.74 ± 0.02	0.76 ± 0.02	-2.37 ± 0.03
V52 H73				-1.14 ± 0.04	0.87 ± 0.11	-1.56 ± 0.05
L52 H73	1.34 ± 0.06	0.56 ± 0.10	1.83 ± 0.08	-0.55 ± 0.04	0.88 ± 0.07	-0.75 ± 0.05
I52 H73				-0.45 ± 0.02	0.93 ± 0.04	-0.62 ± 0.03

[a] *m*-Values and pK_C(0) values were obtained by fitting plots of pK_C versus [gdnHCl] to the equation $pK_C = pK_C(0) - \{m/(\ln(10)RT)\}$[gdnHCl], where *R* is the universal gas constant and *T* is temperature in degrees Kelvin. $\Delta G_u(H_2O)$ for partial unfolding was obtained from pK_C(0) through the relationship $\Delta G_u(H_2O) = \ln(10)RTpK_C(0)$. [b] Data from ref *20*. [c] For the A52 H73 variant, the 0 M gdnHCl pK_C(H73) data point was not used in the fit to the equation in footnote a because it significantly deviated from the line produced by the other four data points (see Figure 5). Inclusion of this data point decreases *m* to 1.33 ± 0.12 and pK_C(0) to 0.85 ± 0.04, giving $\Delta G_u(H_2O) = 1.16 \pm 0.05$. For the T52 H73 variant, the 0 M gdnHCl pK_C(H73) data point was not included in the fit to the equation in footnote a because of the large error bars on this data point (see Table 2).

Table 4: Changes in Free Energy, $\Delta\Delta G$, for Global versus Partial Unfolding Caused by Mutations at Position 52[a]

variant	$\Delta\Delta G_{global}$ (kcal/mol)	$\Delta\Delta G_{His73}$ (kcal/mol)	$\Delta\Delta G_{Lys79}$ (kcal/mol)
A52 H73	0.83 ± 0.36	0.91 ± 0.05	0.04 ± 0.13
T52 H73	1.34 ± 0.28	1.7 ± 0.3	0.60 ± 0.08
V52 H73	2.47 ± 0.34		1.41 ± 0.10
L52 H73	3.28 ± 0.54	1.46 ± 0.09	2.22 ± 0.10
I52 H73	3.47 ± 0.34		2.35 ± 0.08

[a] $\Delta\Delta G$ is calculated by subtracting the $\Delta G_u(H_2O)$ value for the H73 variant from that for the X52 H73 variant. Therefore, a positive $\Delta\Delta G$ indicates stabilization relative to the H73 variant.

readily discernible in the A_{695} versus pH data. This calculation indicates that $\Delta\Delta G_{His73}$ at the lower limit for these two variants is similar to $\Delta\Delta G_{global}$.

For the L52 H73 variant, $\Delta\Delta G_{global}$ is much larger than $\Delta\Delta G_{His73}$ (Table 4). As discussed above, the L52 mutation appears to perturb the nature of the His 73 alkaline conformer causing this discrepancy.

For the Lys 79 alkaline conformational transition, $\Delta\Delta G_{Lys79}$ is significantly lower than $\Delta\Delta G_{global}$, for all variants. For the A52 H73 and T52 H73 variants, where data for unfolding to both alkaline conformers is available, $\Delta\Delta G_{His73}$ is much larger than $\Delta\Delta G_{Lys79}$. As noted above, on the basis of *m*-value data, formation of the Lys 79 alkaline conformer is unlikely to correspond to unfolding of the entire Red substructure but presumably corresponds to unfolding of some subset of this substructure. Thus, the results indicate that when unfolding does not correspond well to a natural substructure, the energy coupling between substructures is incomplete, causing a partial decoupling of the sequential unfolding pathway outlined in the Introduction. It is interesting to note in Figure 2 that the region of the Red substructure around Lys 79 contacts the N-yellow substructure primarily between amino acids 45 and 50. Perhaps the Lys 79 alkaline state can form with only partial unfolding of the N-yellow substructure, leading to a fractional propagation of stabilization energy.

Implications for the Unfolding Pathway of Cytochrome c. In the initial report on the N-yellow substructure, the authors indicated that their data could not distinguish between sequential and independent unfolding of the N-yellow and Red substructures (*10*). As discussed above, the available data indicate that the His 73 alkaline conformer of cytochrome *c* corresponds to unfolding of the Red substructure (*18*−*21*, *25*). We observe that mutations at position 52 in the N-yellow substructure impart a similar amount of stabilization energy to the portion of the protein unfolded by the His 73 alkaline conformer as to the Blue substructure (global unfolding). This result indicates that the N-yellow substructure unfolds in advance of, not independently of, the Red substructure. So, cytochrome *c* appears to unfold sequentially from the least to the most stable substructure. The NMR structure of the Lys 73 alkaline conformer of iso-1-cytochrome *c* (*47*) shows substantial disruption of the Red substructure. The data also indicate that the portion of the protein corresponding to the N-yellow substructure is not well-defined either, indicating that it may be disrupted, as well.

It is interesting to speculate about the effect of the L52 mutation. It is possible that the L52 mutation either has decoupled unfolding of the N-yellow and Red substructures so that they unfold independently or has inverted the stability of the Red and N-yellow substructures. If the latter is true, it suggests that single-site mutations can affect the ordering of adjacent excited states of a protein. Further research will be necessary to determine whether this is the case for the L52 H73 variant. A similar rearrangement of the unfolding pathway is not evident for the Lys 79 alkaline transition of the L52 H73 variant (see Tables 3 and 4). As discussed above, this result may be due to a relaxation of the requirement for full unfolding of the N-yellow substructure in the case of partial unfolding mediated by Lys 79−heme ligation.

SUMMARY

Stabilizing mutations at position 52 in the least stable N-yellow substructure have similar stabilizing effects on the Red (unfolding to the His 73 alkaline conformer) and Blue (global unfolding) substructures of cytochrome *c*. This result is consistent with upward propagation of stabilizing energy from lower energy to higher energy substructures as expected for sequential unfolding of cytochrome *c* from the least to the most stable substructure. The results for the L52 H73 variant suggest that single-site mutations can modify the

nature of protein substructures. The observation that the propagation of stabilization energy, from the N-yellow substructure to the portion of cytochrome *c* unfolded in the Lys 79 alkaline conformer, is only partial indicates that when unfolding does not correspond to a natural substructure, full energetic coupling resulting from sequential unfolding of the protein's substructures no longer occurs.

SUPPORTING INFORMATION AVAILABLE

Figure S1 showing A_{695} versus CD-monitored gdnHCl denaturation of the T52 H73, V52 H73, and L52 H73 variants and Figure S2 showing the gdnHCl-dependence of the alkaline conformational transition for the T52 H73 and V52 H73 variants. This material is available free of charge via the Internet at http://pubs.acs.org.

REFERENCES

1. Dill, K. A. (1990) Dominant forces in protein folding, *Biochemistry 29*, 7133−7155.
2. Pace, C. N., Shirley, B. A., McNutt, M., and Gajiwala, K. (1996) Forces contributing to the conformational stability of proteins, *FASEB J. 10*, 75−83.
3. Suel, G. M., Lockless, S. W., Wall, M. A., and Ranganathan, R. (2003) Evolutionarily conserved networks of residues mediate allosteric communication in proteins, *Nat. Struct. Biol. 10*, 59−69.
4. Englander, S. W., Mayne, L., and Rumbley, J. N. (2002) Submolecular cooperativity produces multi-state protein unfolding and refolding, *Biophys. Chem. 101*−*102*, 57−65.
5. Chamberlain, A. K., and Marqusee, S. (2000) Comparison of equilibrium and kinetic approaches for determining protein folding mechanisms, *Adv. Protein Chem. 53*, 283−328.
6. Bai, Y., Sosnick, T. R., Mayne, L., and Englander, S. W. (1995) Protein folding intermediates: Native-state hydrogen exchange, *Science 269*, 192−197.
7. Xu, Y., Mayne, L., and Englander, S. W. (1998) Evidence for an unfolding and refolding pathway in cytochrome *c*, *Nat. Struct. Biol. 5*, 774−778.
8. Milne, J. S., Xu, Y., Mayne, L. C., and Englander, S. W. (1999) Experimental study of the protein folding landscape: Unfolding reactions in Cytochrome *c*, *J. Mol. Biol. 290*, 811−822.
9. Hoang, L., Bédard, S., Krishna, M. M. G., Lin, Y., and Englander, S. W. (2002) Cytochrome *c* folding pathway: Kinetic native state hydrogen exchange, *Proc. Natl. Acad. Sci. U.S.A. 99*, 12173−12178.
10. Krishna, M. M. G., Lin, Y., Rumbley, J. N., and Englander, S. W. (2003) Cooperative omega loops in cytochrome *c*: Role in folding and function, *J. Mol. Biol. 331*, 29−36.
11. Krishna, M. M. G., Lin, Y., Mayne, L., and Englander, S. W. (2003) Intimate view of a kinetic protein folding intermediate: Residue-resolved structure, interaction, stability, folding and unfolding rates, homogeneity, *J. Mol. Biol. 334*, 501−513.
12. Baxter, S. M., and Fetrow, J. S. (1999) Hydrogen exchange behavior of [U-^{15}N]-labeled oxidized and reduced iso-1-cytochrome *c*, *Biochemistry 38*, 4493−4503.
13. Fetrow, J. S., and Baxter, S. M. (1999) Assignment of ^{15}N chemical shifts and ^{15}N relaxation measurements for oxidized and reduced iso-1-cytochrome *c*, *Biochemistry 38*, 4480−4492.
14. Marmorino, J. L., Auld, D. S., Betz, S. F., Doyle, D. F., Young, G. B., and Pielak, G. J. (1993) Amide proton exchange rates of oxidized and reduced *Saccharomyces cerevisiae* iso-1-cytochrome *c*, *Protein Sci. 2*, 1966−1974.
15. Goedken, E. R., and Marqusee, S. (2001) Native-state energetics of a thermostabilized variant of Ribonuclease HI, *J. Mol. Biol. 314*, 863−871.
16. Spudich, G., Lorenz, S., and Marqusee, S. (2002) Propagation of a single destabilizing mutation throughout the *Escherichia coli* ribonuclease HI native state, *Protein Sci. 11*, 522−528.
17. Luque, I., Leavitt, S. A., and Freire, E. (2002) The linkage between protein folding and functional cooperativity: Two sides of the same coin, *Annu. Rev. Biophys. Biomol. Struct. 31*, 235−256.
18. Godbole, S., Dong, A., Garbin, K., and Bowler, B. E. (1997) A lysine 73 → histidine variant of yeast iso-1-cytochrome *c*: Evidence for a native-like intermediate in the unfolding pathway and implications for *m* value effects, *Biochemistry 36*, 119−126.
19. Godbole, S., and Bowler, B. E. (1999) Effect of pH on formation of a nativelike intermediate on the unfolding pathway of a Lys 73 → His variant of yeast iso-1-cytochrome *c*, *Biochemistry 38*, 487−495.
20. Nelson, C. J., and Bowler, B. E. (2000) pH dependence of formation of a partially unfolded state of a Lys 73 → His variant of iso-1-cytochrome *c*: Implications for the alkaline conformational transition of cytochrome *c*, *Biochemistry 39*, 13584−13594.
21. Nelson, C. J., LaConte, M. J., and Bowler, B. E. (2001) Direct detection of heat and cold denaturation for partial unfolding of a protein, *J. Am. Chem. Soc. 123*, 7453−7454.
22. Rosell, F. I., Ferrer, J. C., and Mauk, A. G. (1998) Proton-linked protein conformational switching: Definition of the alkaline conformational transition of yeast iso-1-ferricytochrome *c*, *J. Am. Chem. Soc. 120*, 11234−11245.
23. Martinez, R. M., and Bowler, B. E. (2004) Proton-mediated dynamics of the alkaline conformational transition of yeast iso-1-cytochrome *c*, *J. Am. Chem. Soc. 126*, 6751−6758.
24. Wilson, M. T., and Greenwood, C. (1996) The alkaline transition in ferricytochrome *c*, in *Cytochrome c: A Multidisciplinary Approach* (Scott, R. A., and Mauk, A. G., Eds) pp 611−634, University Science Books, Sausalito, CA.
25. Hoang, L., Maity, H., Krishna, M. M. G., Lin, Y., and Englander, S. W. (2003) Folding units govern the cytochrome *c* alkaline transition, *J. Mol. Biol. 331*, 37−43.
26. Das, G., Hickey, D. R., McLendon, D., McLendon, G., and Sherman, F. (1989) Dramatic thermostabilization of yeast iso-1-cytochrome *c* by an asparagine → isoleucine replacement at position 57, *Proc. Natl. Acad. Sci. U.S.A. 86*, 496−499.
27. Hickey, D. R., Berghuis, A. M., Lafond, G., Jaeger, J. A., Cardillo, T. S., McLendon, D., Das, G., Sherman, F., Brayer, G. D., and McLendon, G. (1991) Enhanced thermodynamic stabilities of yeast iso-1-cytochromes *c* with amino acid replacements at positions 52 and 102, *J. Biol. Chem. 266*, 11686−11694.
28. Linske-O'Connell, L. I., Sherman, F., and McLendon, G. (1995) Stabilizing amino acid replacements at position 52 in yeast iso-1-cytochrome *c*: In vivo and in vitro effects, *Biochemistry 34*, 7094−7102.
29. Berghuis, A. M., and Brayer, G. D. (1992) Oxidation state-dependent conformational changes in cytochrome *c*, *J. Mol. Biol. 223*, 959−976.
30. Sobolev, V., Sorokine, A., Lusky, J., and Abola, E. E. (1999) Automated analysis of interatomic contacts in proteins, *Bioinformatics 15*, 327−332.
31. Smith, C. R., Mateljevic, N., and Bowler, B. E. (2002) Effects of topology and excluded volume on protein denatured state conformational properties, *Biochemistry 41*, 10173−10181.
32. Deng, W. P. D., and Nickoloff, J. A. (1992) Site-directed mutagenesis of virtually any plasmid by eliminating a unique site, *Anal. Biochem. 200*, 81−88.
33. Ito, H., Fukada, Y., Murata, K., and Kimura, K. (1983) Transformation of intact yeast cells treated with alkali cations, *J. Bacteriol. 153*, 163−168.
34. Bowler, B. E., May, K., Zaragoza, T., York, P., Dong, A., and Caughey, W. S. (1993) Destabilizing effects of replacing a surface lysine of cytochrome *c* with aromatic amino acids: Implications for the denatured state, *Biochemistry 32*, 183−190.
35. Strathern, J. N., and Higgins, D. R. (1991) Recovery of plasmids from yeast into *Escherichia coli*: shuttle vectors, *Methods Enzymol. 194*, 319−329.
36. Bowler, B. E., Dong, A., and Caughey, W. S. (1994) Characterization of the guanidine hydrochloride-denatured state of iso-1-cytochrome *c* by infrared spectroscopy, *Biochemistry 33*, 2402−2408.
37. Pace, C. N. (1986) Determination and analysis of urea and guanidine hydrochloride denaturation curves, *Methods Enzymol. 26*, 266−280.
38. Herrmann, L., Bowler, B. E., Dong, A., and Caughey, W. S. (1995) The effects of hydrophilic to hydrophobic surface mutations on the denatured state of iso-1-cytochrome *c*: Investigation of aliphatic residues, *Biochemistry 34*, 3040−3047.

39. Godbole, S., Hammack, B., and Bowler, B. E. (2000) Measuring denatured state energetics: Deviations from random coil behavior and implications for the folding of iso-1-cytochrome *c*, *J. Mol. Biol. 296*, 217−228.
40. Santoro, M. M., and Bolen, D. W. (1988) Unfolding free energy determined by the linear extrapolation method. 1. Unfolding of phenylmethanesulfonyl α-chymotrypsin using different denaturants, *Biochemistry 27*, 8063−8068.
41. Moore, G. R., and Pettigrew, G. (1990) *Cytochrome c: Evolutionary, Structural and Physicochemical Aspects*, pp 69−70, Springer-Verlag, New York.
42. Zhang, M.-M., Ford, C. D., and Bowler, B. E. (2004) Estimation of the compaction of the denatured state by a protein variant involved in a reverse hydrophobic effect, *Protein J. 23*, 119−126.
43. Pace, C. N. (1975) The stability of globular proteins, *CRC Crit. Rev. Biochem. 3*, 1−43.
44. Nozaki, Y., and Tanford, C. (1967) Acid−base titrations in concentrated guanidine hydrochloride. Dissociation constants of the guanidinium ion and of some amino acids, *J. Am. Chem. Soc. 89*, 736−742.
45. Wandschneider, E., and Bowler, B. E. (2004) Conformational properties of the iso-1-cytochrome *c* denatured state: Dependence on guanidine hydrochloride concentration, *J. Mol. Biol. 339*, 185−197.
46. Myers, J. K., Pace, C. N., and Scholtz, J. M. (1995) Denaturant *m* values and heat capacity changes: Relation to changes in accessible surface areas of protein unfolding, *Protein Sci. 4*, 2138−2148.
47. Assfalg, M., Bertini, I., Dolfi, A., Turano, P., Mauk, A. G., Rosell, F. I., and Gray, H. B. (2003) Structural model for an alkaline form of ferricytochrome *c*, *J. Am. Chem. Soc. 125*, 2913−2922.

BI048141R